

Silvio Pantoja G.
Departamento de Oceanografía
Universidad de Concepción

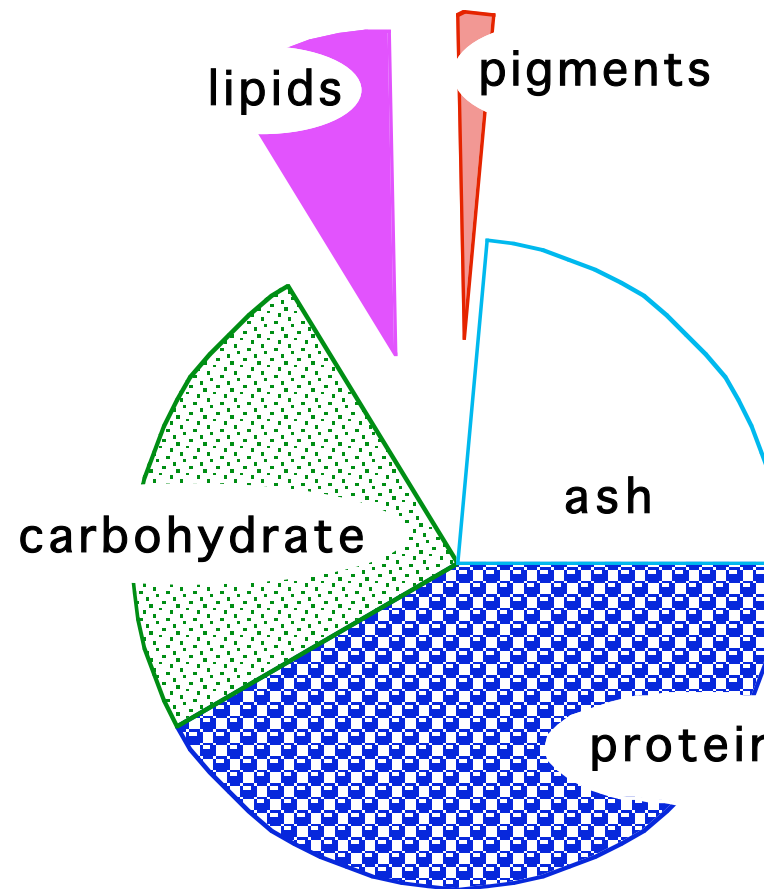
MATERIA ORGÁNICA EN EL OCÉANO. COMPOSICIÓN Y REACCIONES

- Producción fotosintética de materia orgánica
- Composición química de organismos
- Alquenonas como paleo termómetro
- Amino ácidos como herramientas de datación

Para saber más

- S Pantoja, SG Wakeham. 2002. Marine Organic Geochemistry: A General Overview.
- Libes Capítulo
- TI Eginton, DJ Repeta. Marine Organic Geochemistry. 2005

Phytoplankton



Parsons et al. 1961

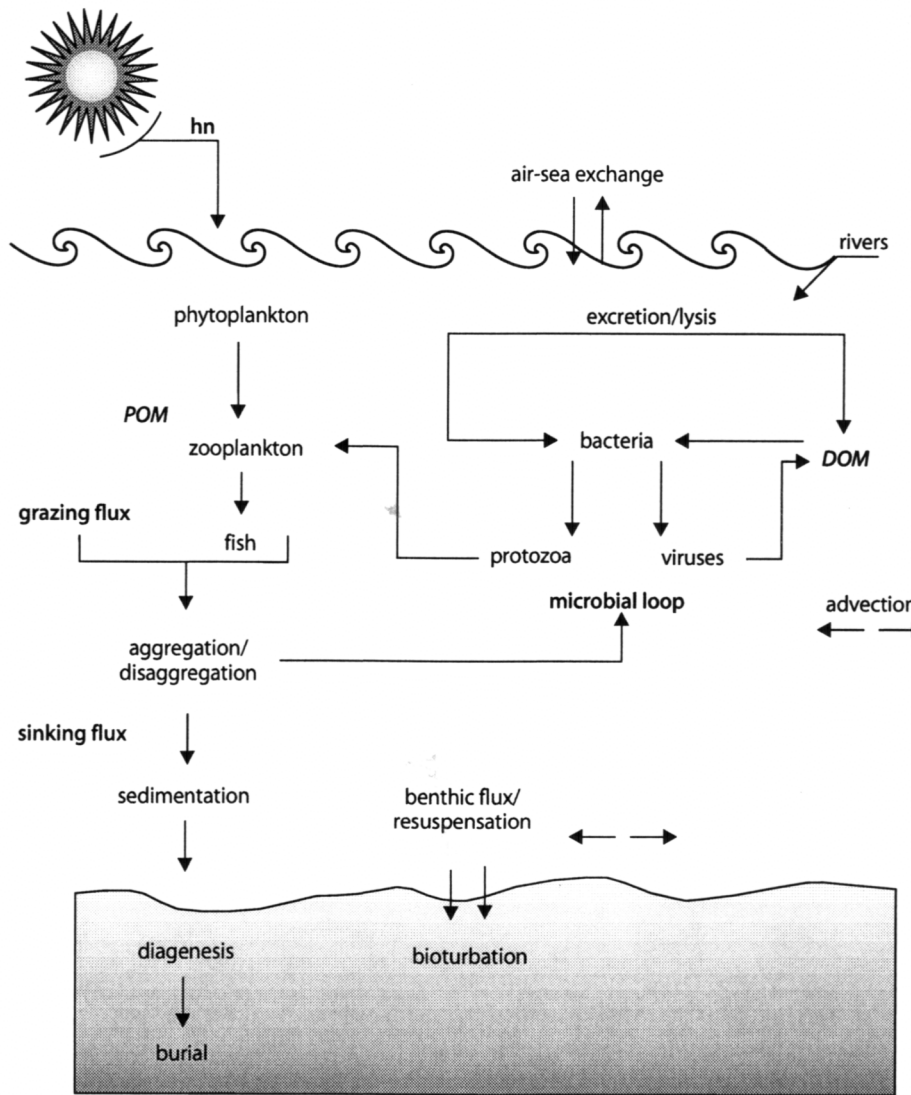
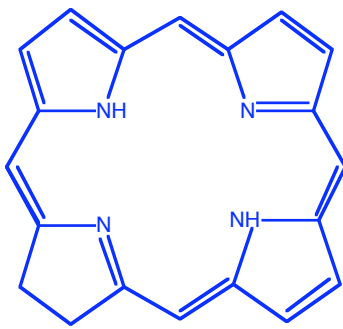
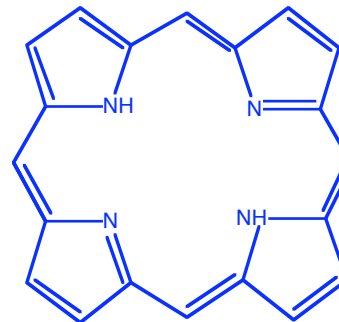


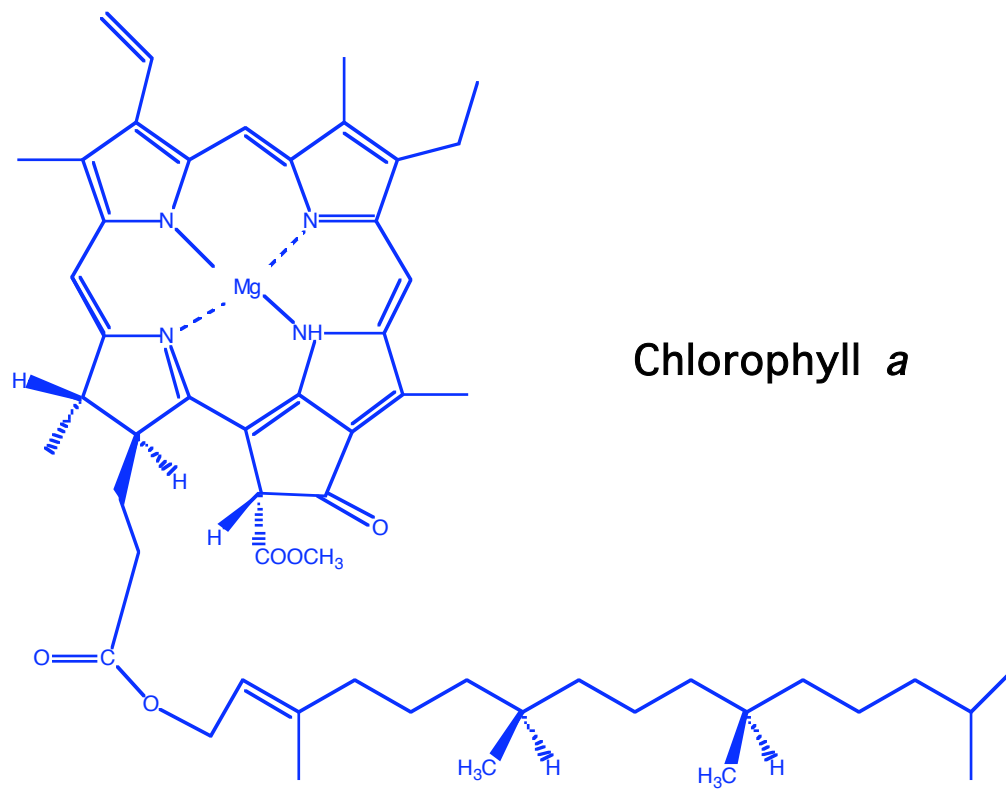
Fig. 2.1. Schematic of biogeochemical cycles in the ocean, showing the grazing food chain, sinking flux, and microbial loop (adapted from Azam 1998)



Chlorin 17,18-Dihydrochlorophyll

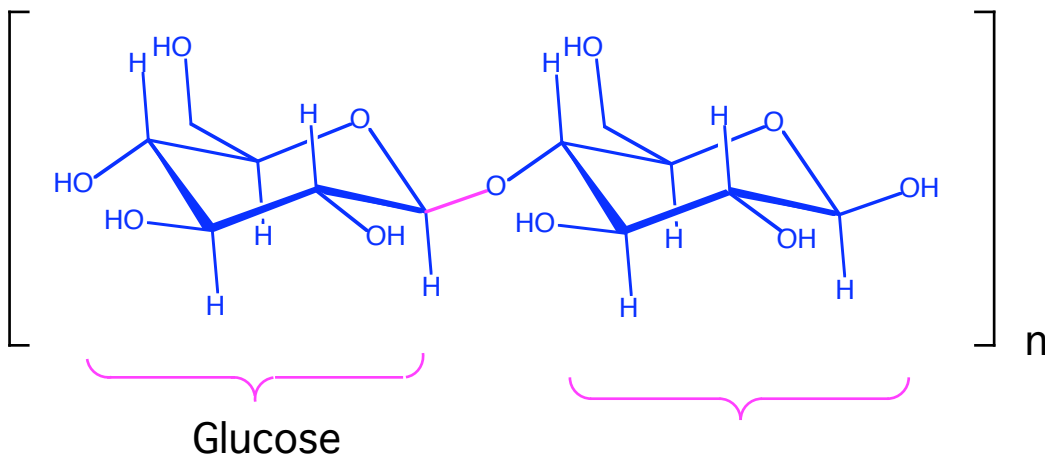


Porphyrin



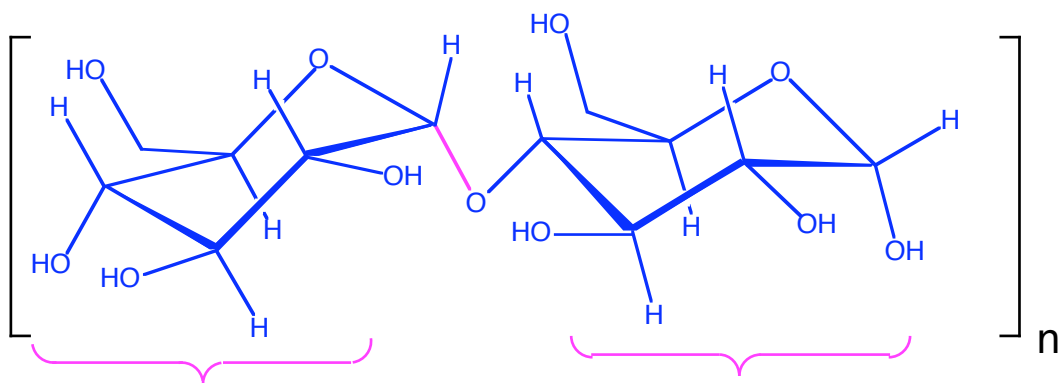
Chlorophyll *a*

CELLULOSE



Glucose

STARCH



OCEANIC PARTICLE SIZE DISTRIBUTION

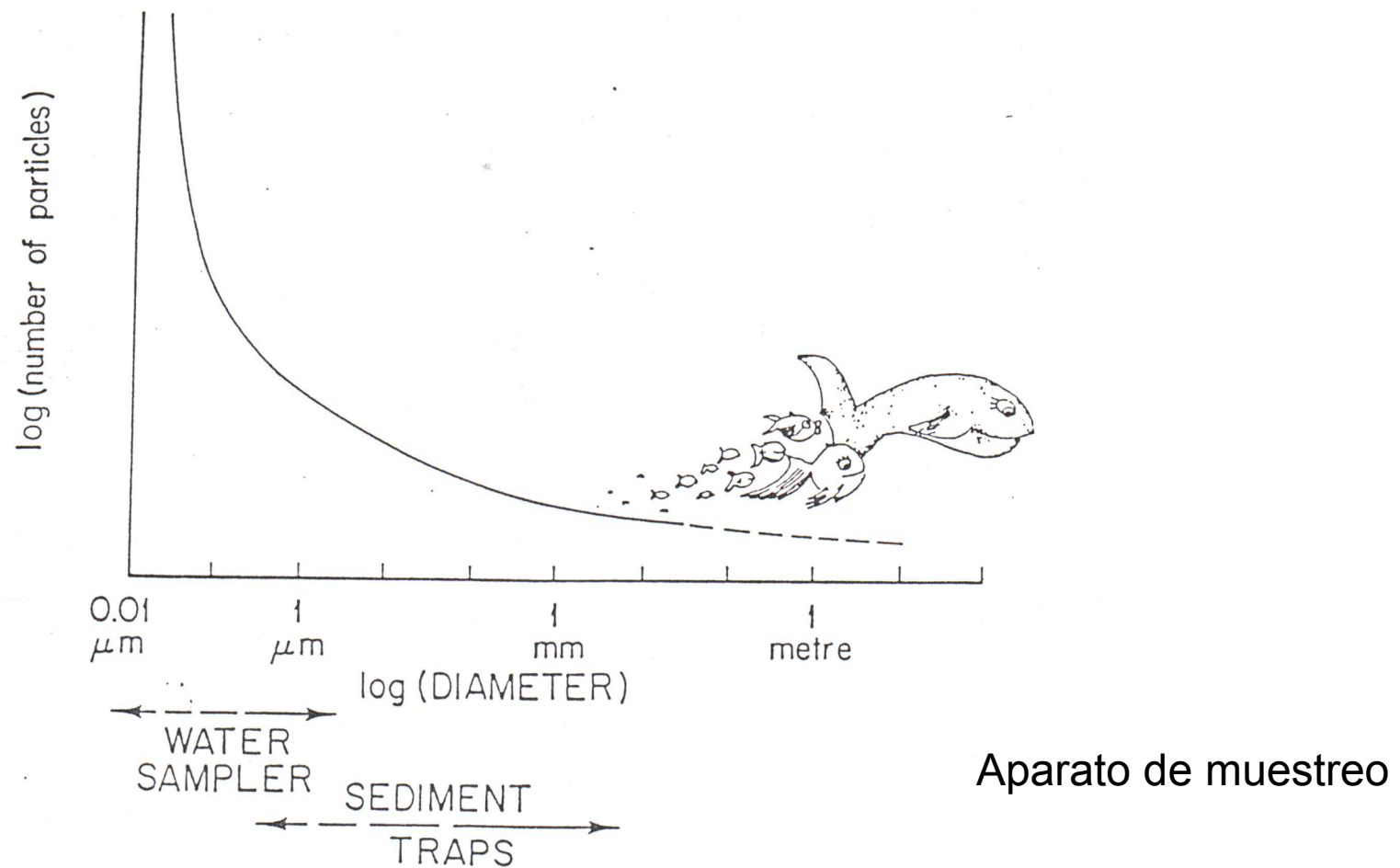


FIG. 49.1. Size distribution of particles in the ocean, including size ranges of particles typically collected by water bottles and sediment traps. (After McCave, 1975.)

McCave, I. N. 1975. Vertical flux of particles in the ocean.
Deep-Sea Research, 22, 491- 502

Organic Carbon Continuum

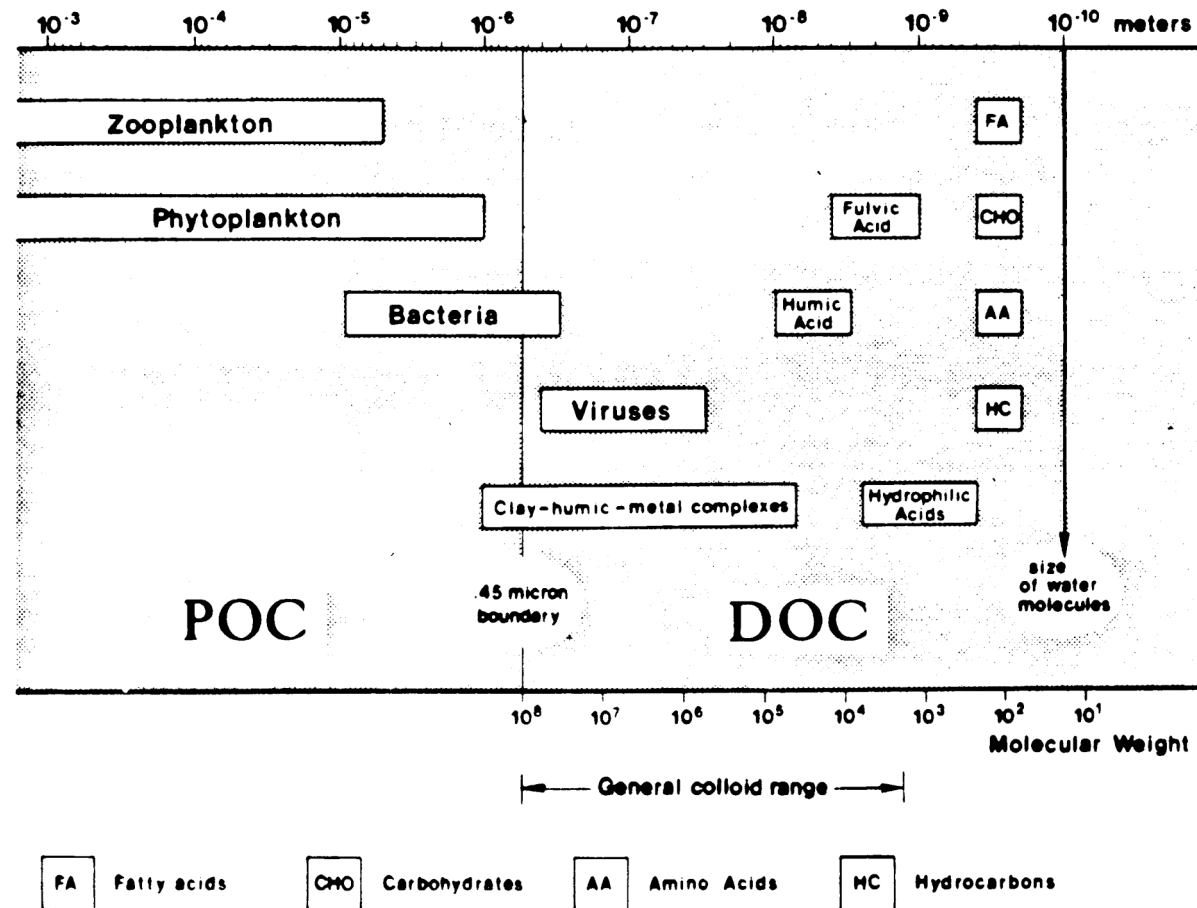
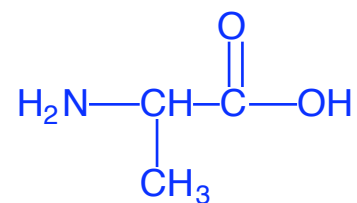


Figure 1. Continuum of particulate and dissolved organic carbon in natural waters.

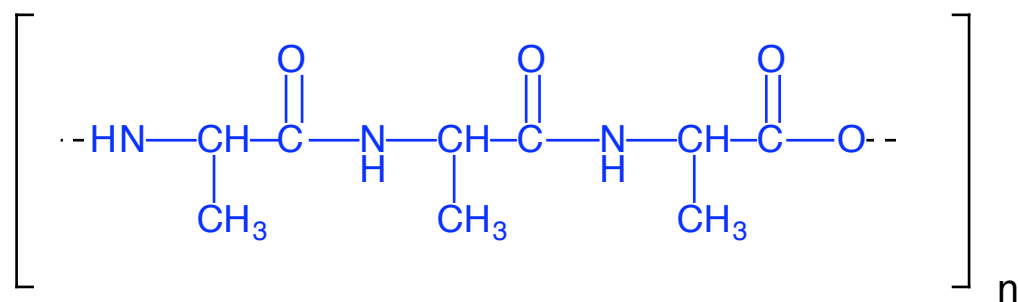
H₂O

Water ≈ 20 Daltons



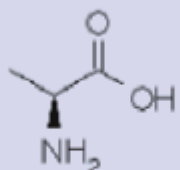
Amino Acid ≈ 130 Daltons

A Protein, up to 600,000 Daltons

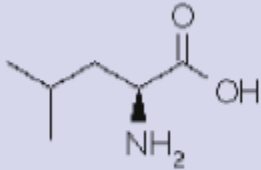


Protein Amino Acids

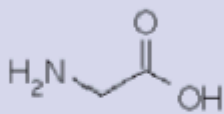
Neutral



Alanine

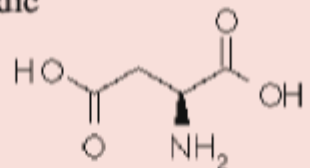


Leucine

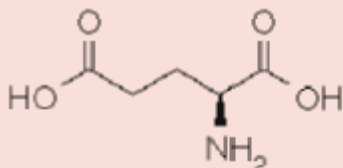


Glycine

Acidic

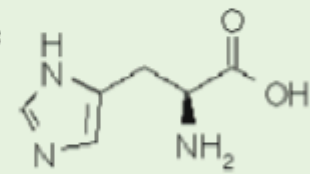


Aspartic acid

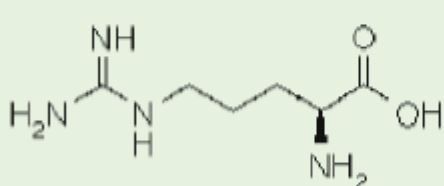


Glutamic acid

Basic

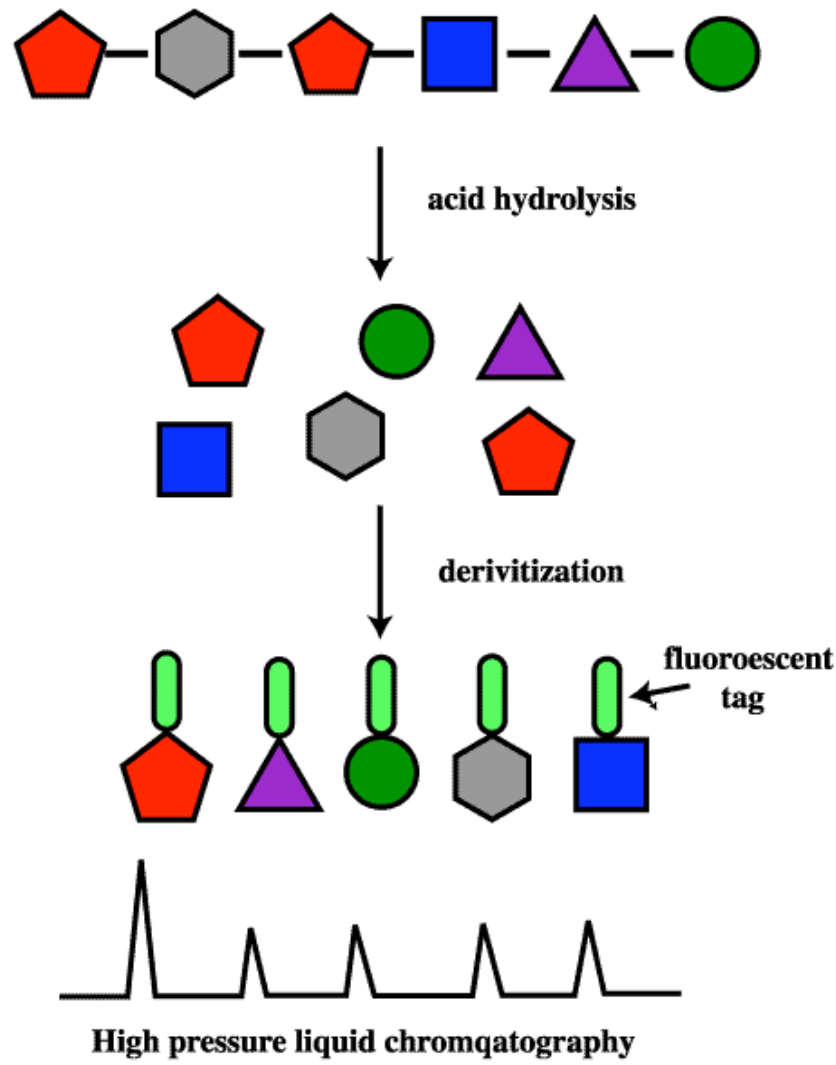


Histidine



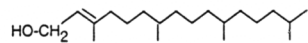
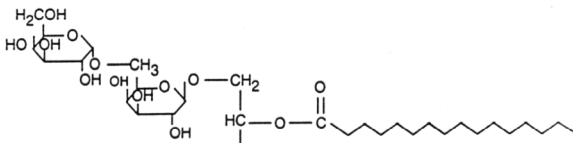
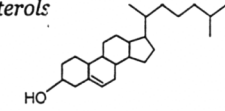
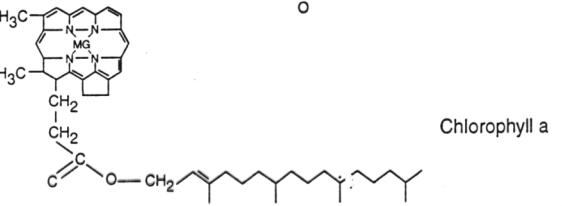
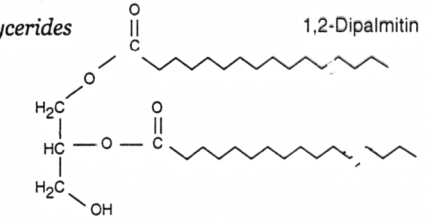
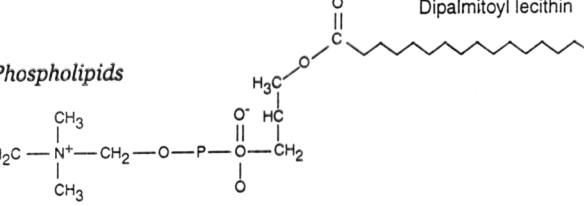
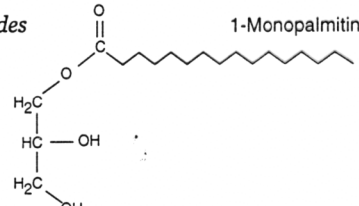
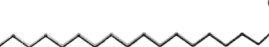
Arginine

Protein Amino Acid Analysis



Lipid class	Structure	Name	Lipid class	Structure	Name
Aliphatic hydrocarbons		n-Nonadecane	Acylated glyceryl esters		Glyceryl-1-hexadecyl ether, 2,3-dipalmitate
Polycyclic aromatic hydrocarbons		Phenanthrene	Triglycerides		Tripalmitin
Wax esters		Hexadecyl palmitate	Free fatty acid		Palmitic acid
Sterol esters		Cholesteryl palmitate	Phthalate esters		Di-2-ethylhexyl phthalate
Short-chain esters		Methyl palmitate	Ketone		2,6,10-trimethyl-pentadecan-2-one

Fig. 2.5 a. Structures of representative lipids

Lipid Class	Structure	Name	Lipid Class	Structure	Name
<i>Free aliphatic alcohols</i>		Phytol	<i>Glycolipids</i>		Digalactosyl diglyceride
<i>Sterols</i>		Cholesterol	<i>Pigments</i>		Chlorophyll a
<i>Diglycerides</i>		1,2-Dipalmitin	<i>Phospholipids</i>		Dipalmitoyl lecithin
<i>Monoglycerides</i>		1-Monopalmitin	<i>Aldhyde</i>		Octadecanal

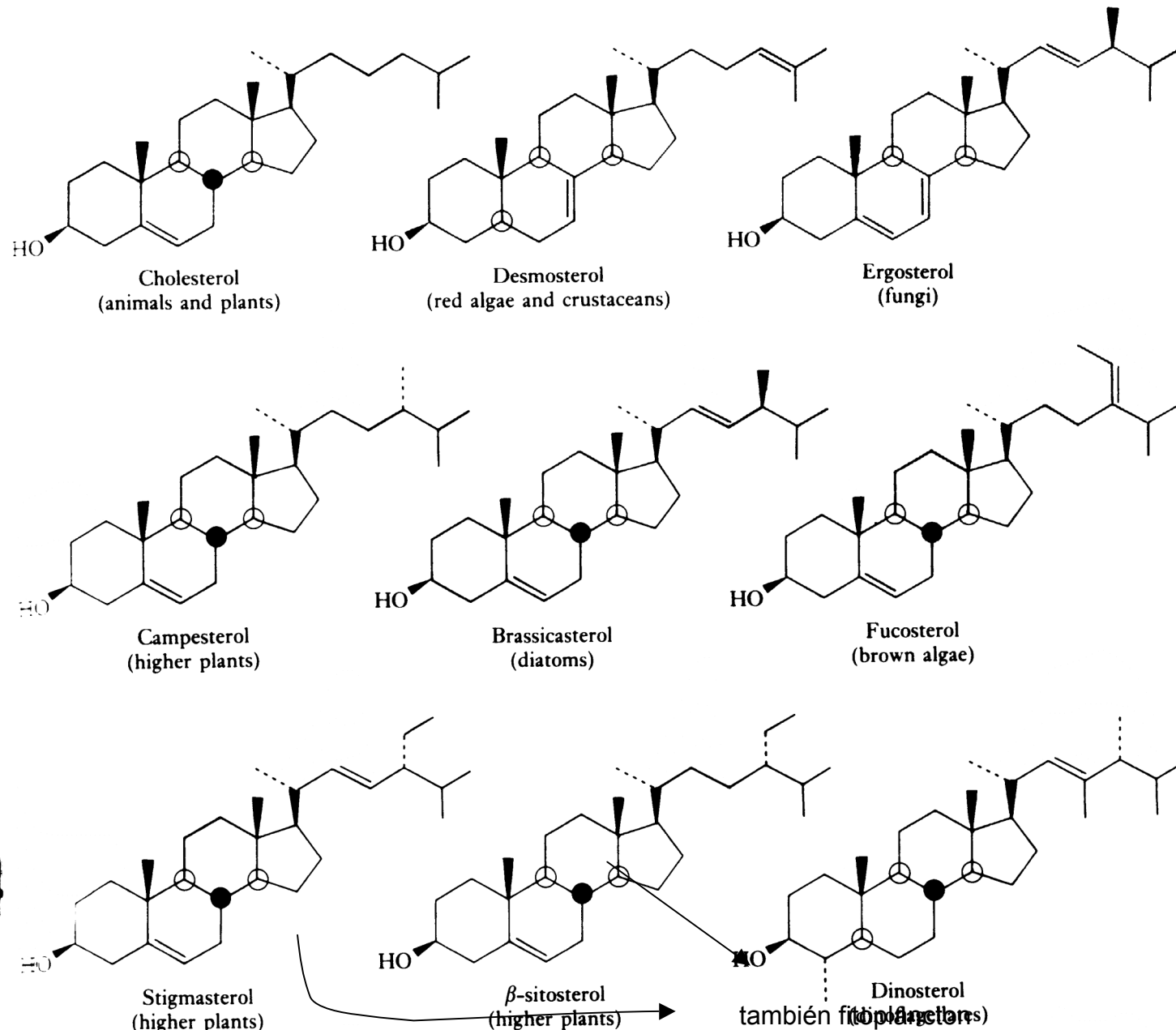
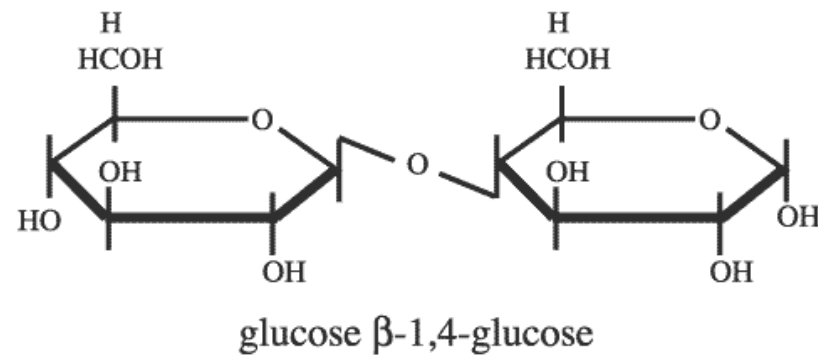
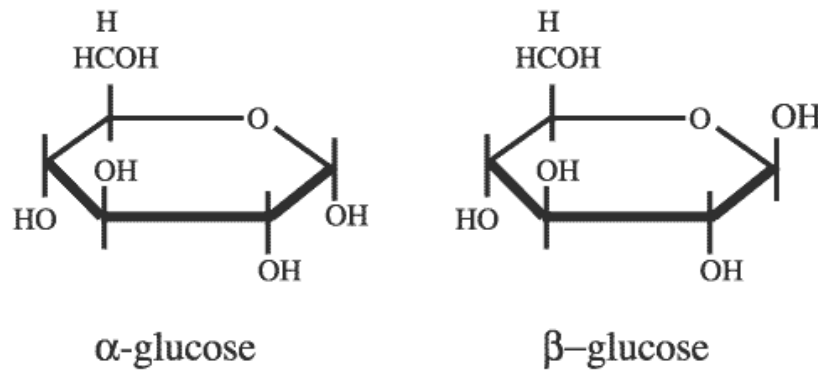


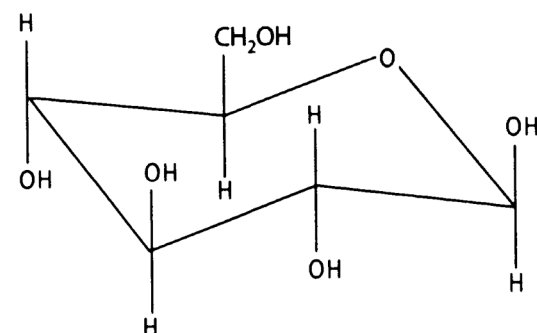
Figure 2.20 Some geochemically important sterols.

Carbohydrate Geometry

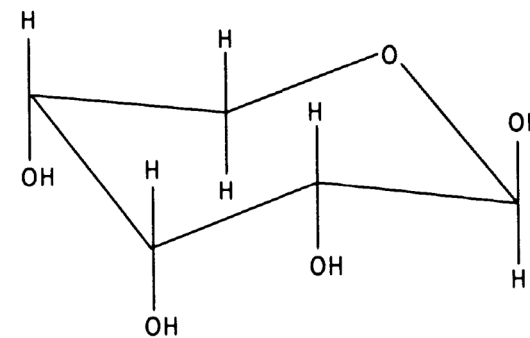


There are many different linkage geometries !!!
 α and β 1,2 1,3 1,6 2,3 1,3,4 1,2,6

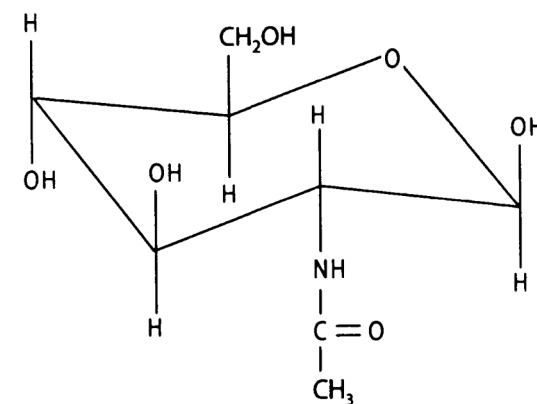
Carbohydrates get their diversity in the linkage pattern,
stereochemistry (α or β) as well as the specific
monosaccharides present



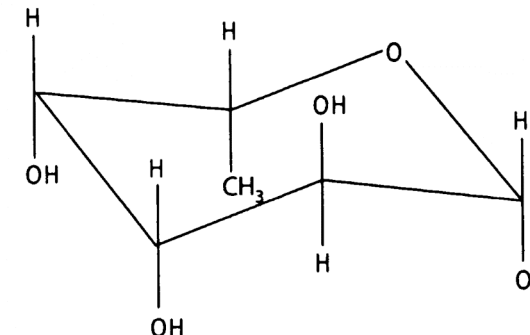
β -D-glucose
(hexose)



β -D-ribose
(pentose)

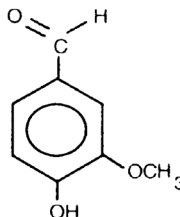
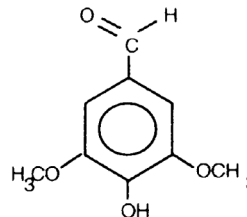
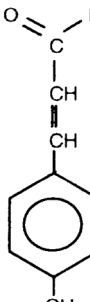
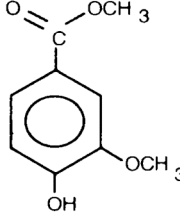
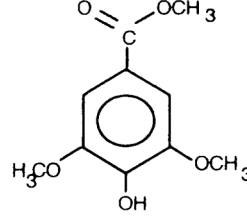
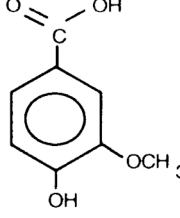
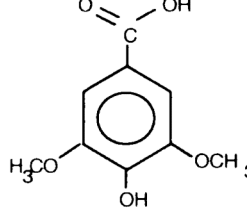
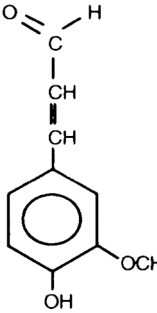


N-acetyl- β -D-glucosamine
(aminosugar)

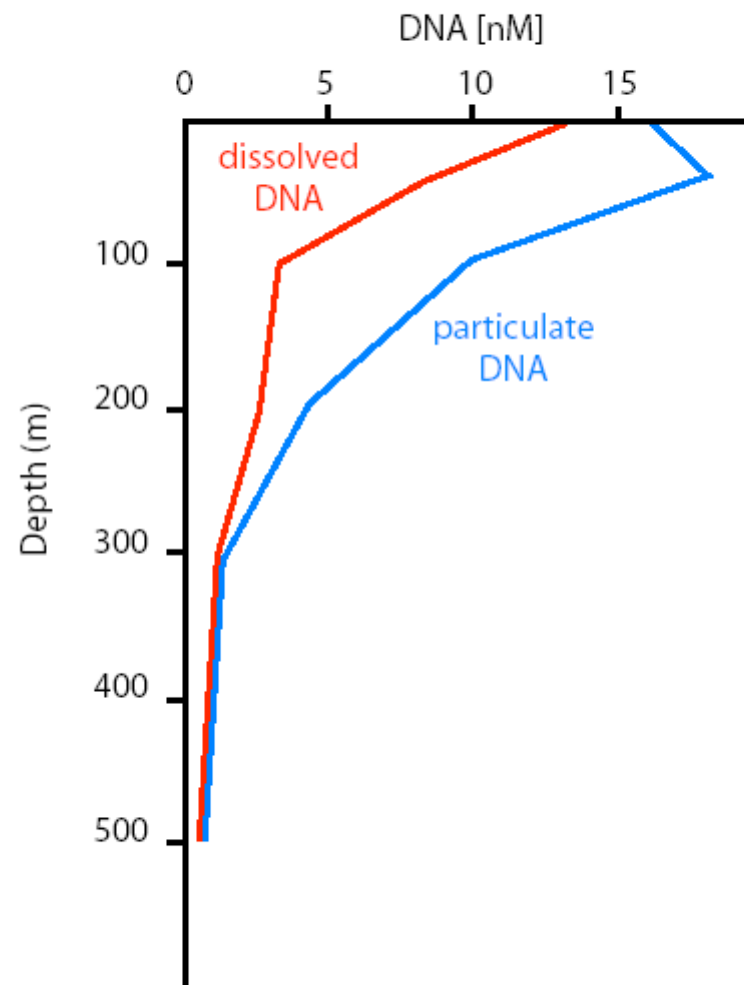


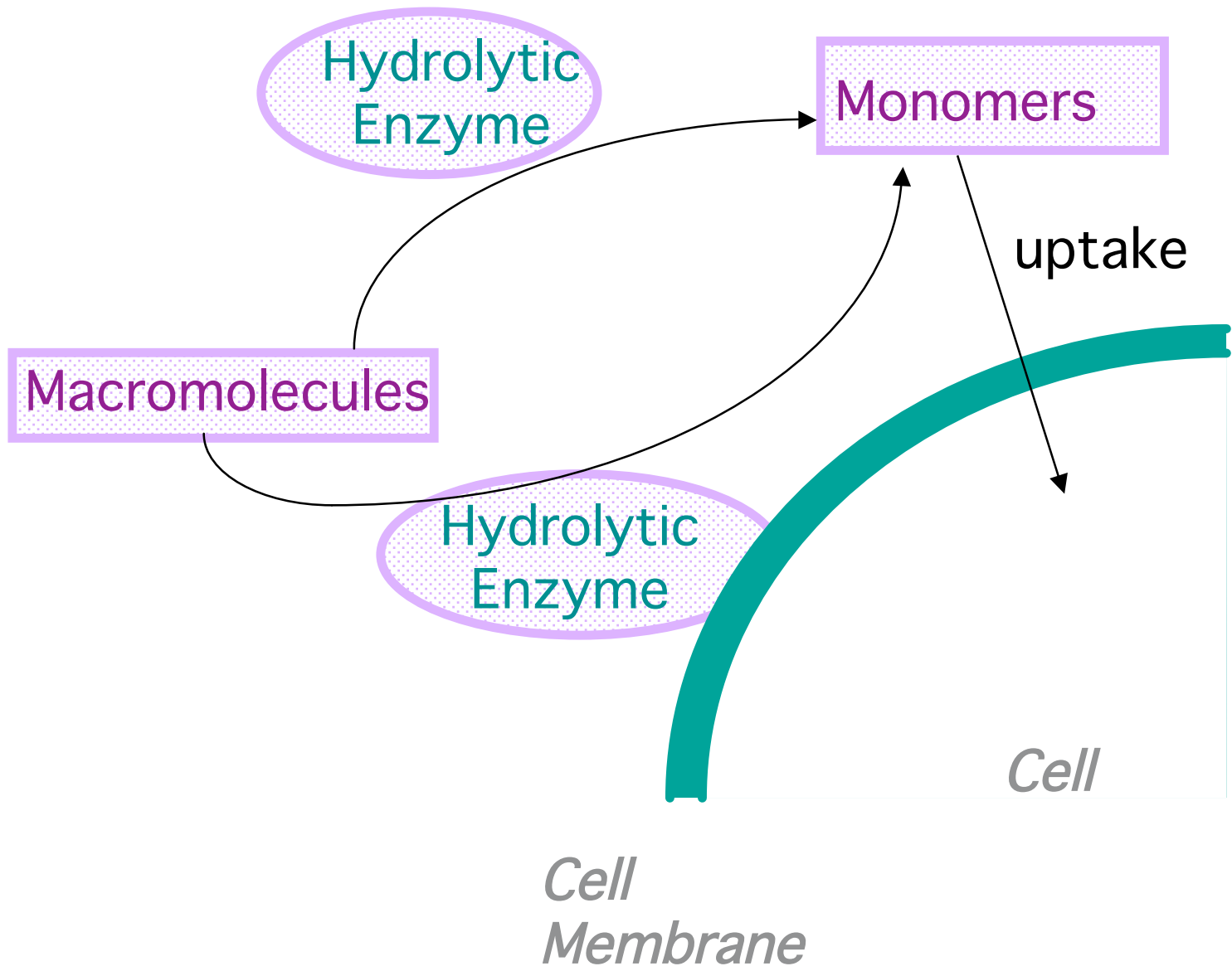
α -D-fucose
(deoxy sugar)

Fig. 2.14. Structure of some common monosaccharides

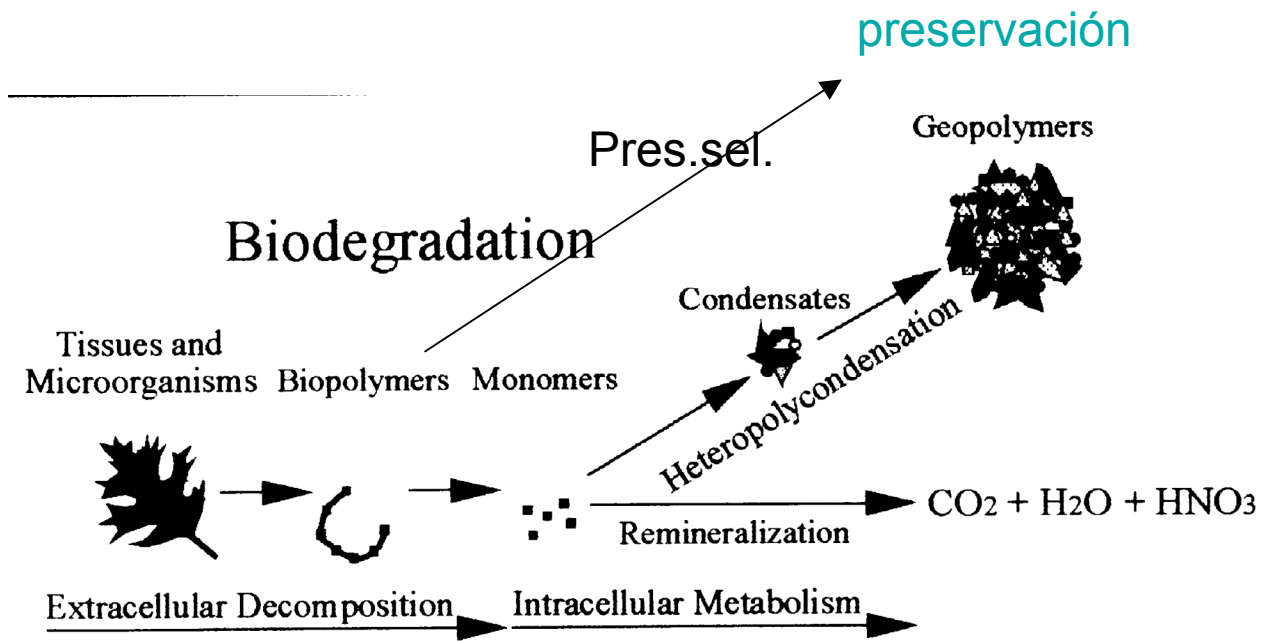
	Vanillyl phenols	Syringyl phenols	Cinnamyl phenols
Aldehydes	 Vanillin	 Syringaldehyde	 p-Coumaric acid
Ketones	 Acetovanillon	 Acetosyringone	
Acids	 Vanillic acid	 Syringic acid	 Ferulic Acid

Distribution of DNA in the Gulf of Mexico
(DeFlaunn et al. 1987)



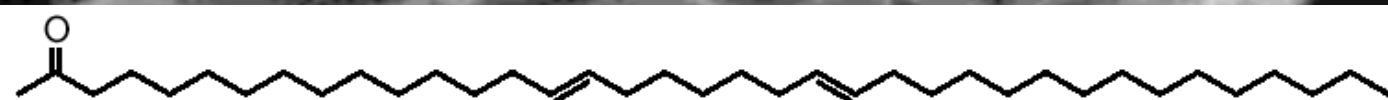


Biodegradación

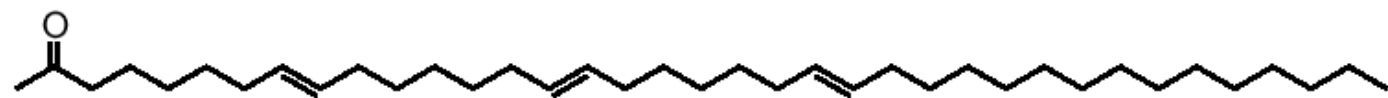


Aplicación 1. Alquenonas

Alkenones ≡ Biomarkers of Specific Haptophytes

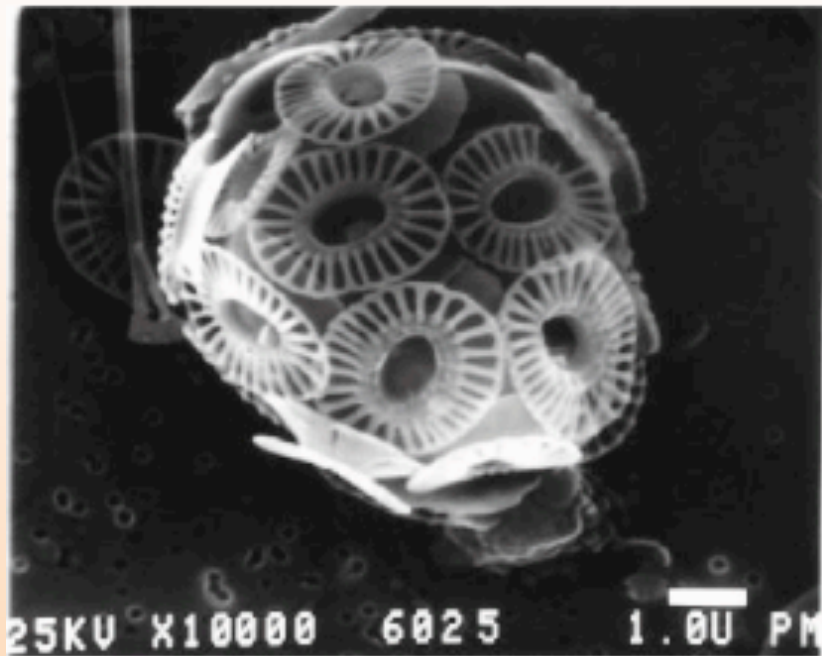


"C_{37:2}," heptatriaconta-15E,22E-dien-2-one



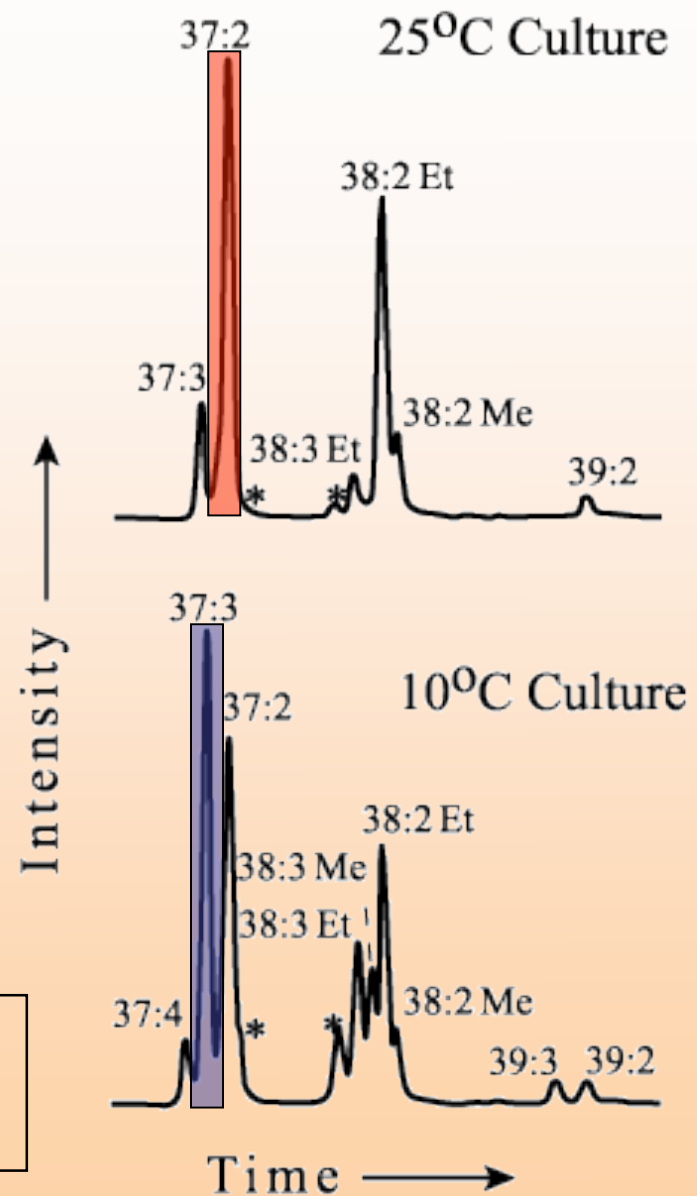
"C_{37:3}," heptatriaconta-8E,15E,22E-trien-2-one

Alkenones



Emiliania huxleyi

$U^K_{37} = [37:2]/([37:2]+[37:3])$
increases with growth temperature



$$U^{K'}_{37} = 0.033T + 0.043$$

(Prahl and Wakeham 1987)

$$U^{K'}_{37} = 0.033T + 0.044$$

(Muller et al. 1998)

$$U^{K'}_{37} = [C_{37:2}] / ([C_{37:2}] + [C_{37:3}])$$

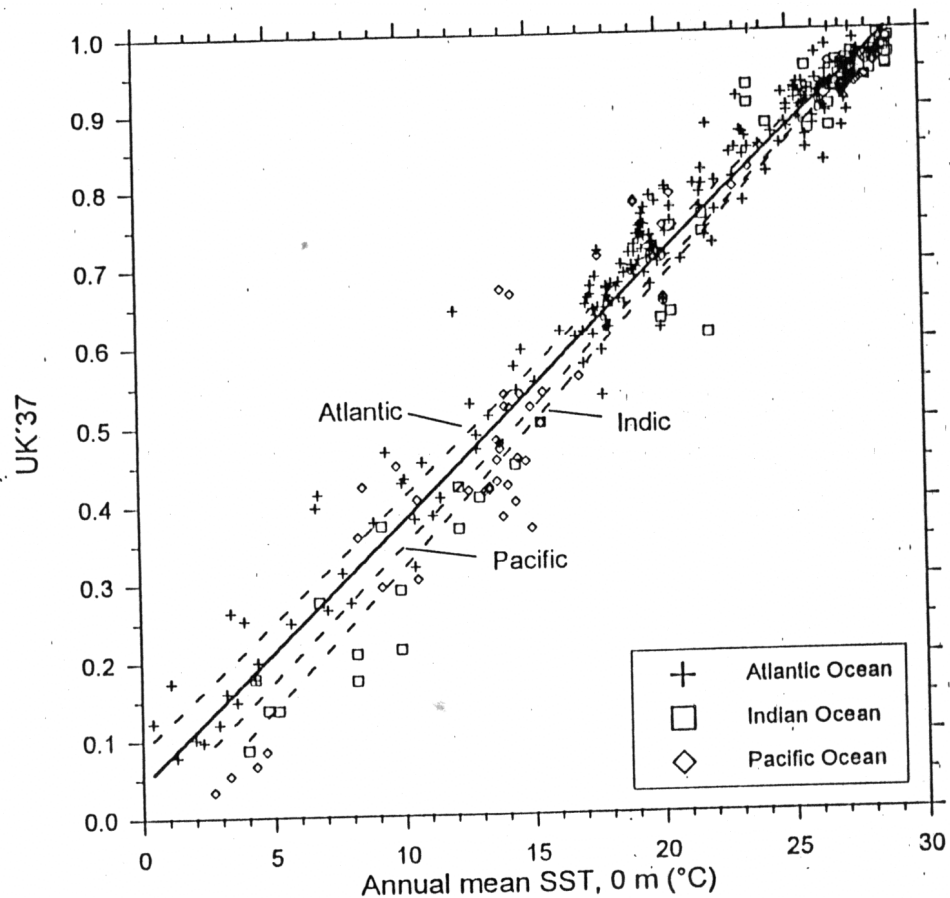
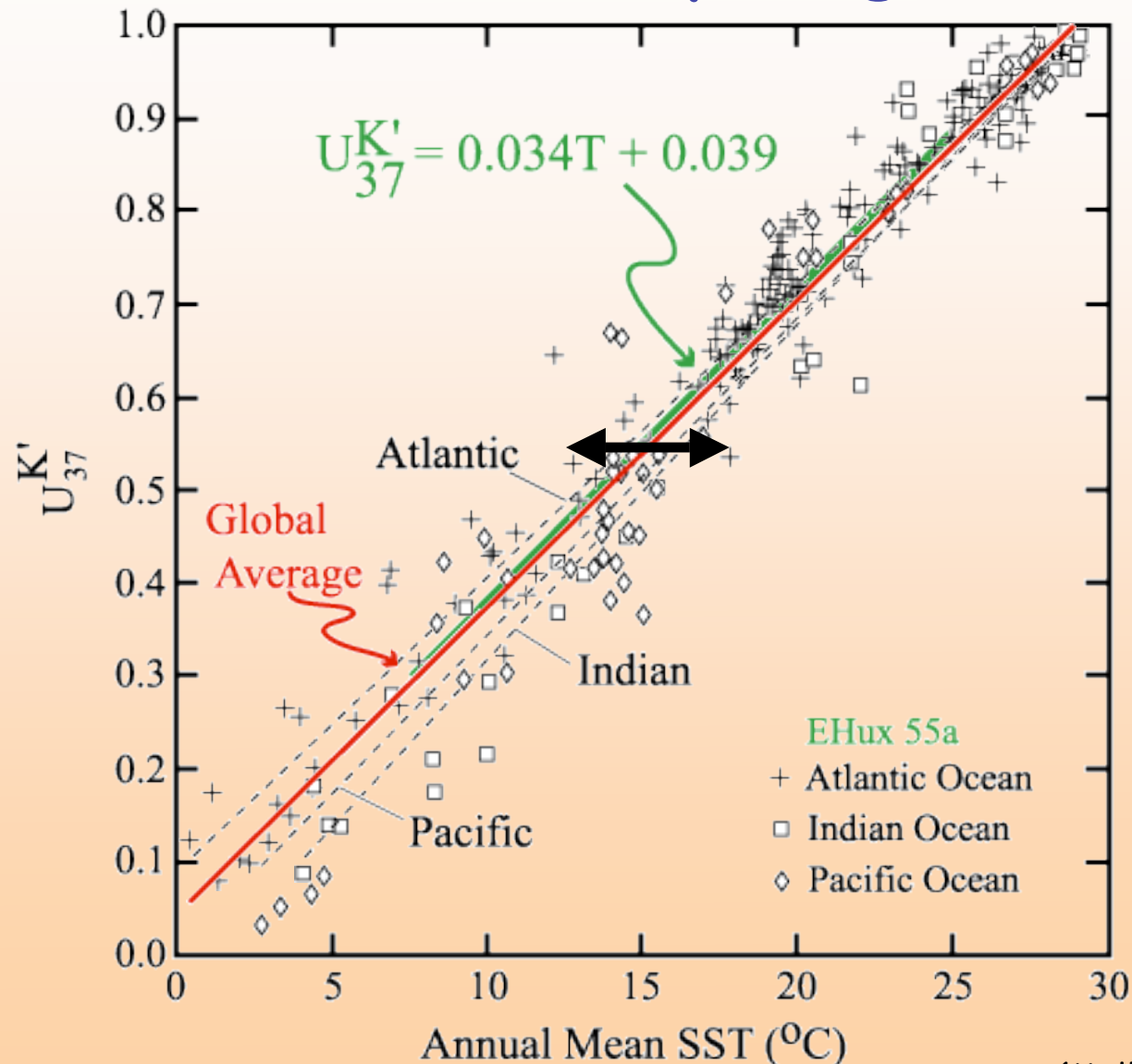


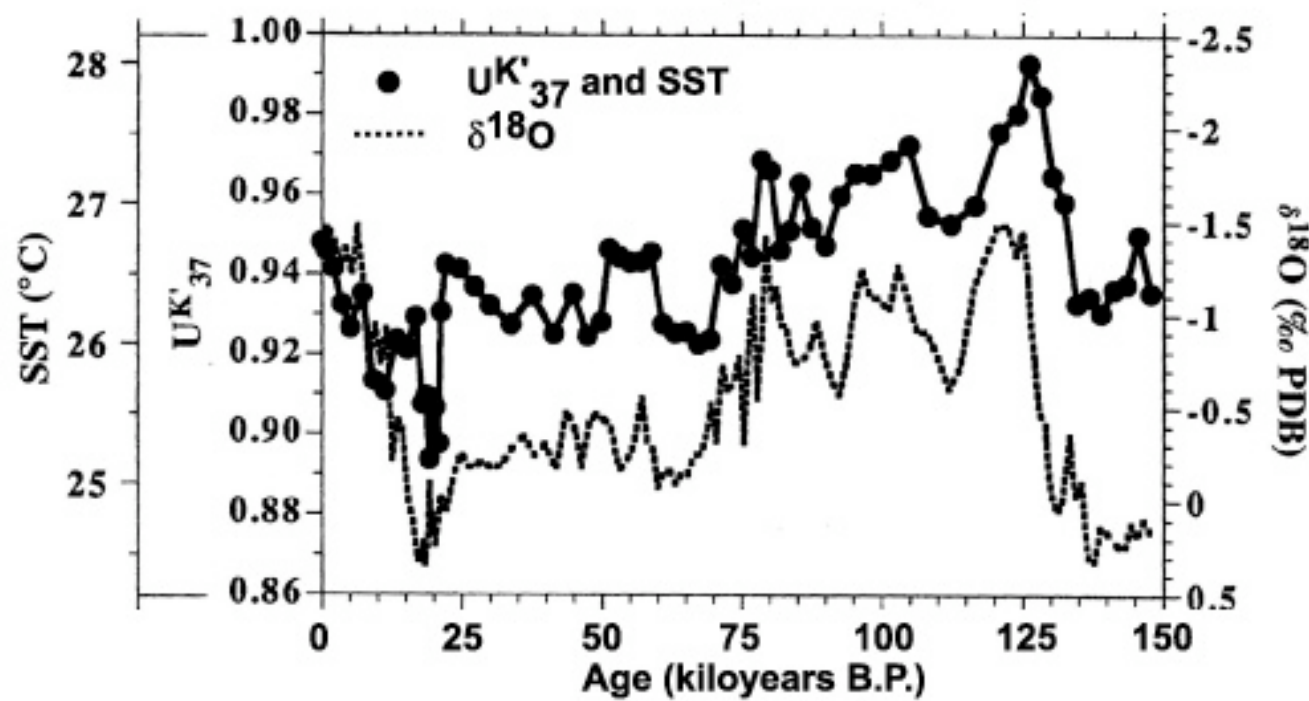
Fig. 7. Relationships between $U^{K'}_{37}$ and annual mean SST (0 m) for surface sediments from the global ocean between 60°S and 60°N . The $U^{K'}_{37}$ data were compiled from the literature (for references see Table 1) and the present study (Appendix), and the temperature data are from Levitus and Boyer (1994) and the COADS archive. The regression parameters for the three oceans (dashed lines) and the global ocean (thick solid line) are given in Table 1. The obtained global core-top calibration ($U^{K'}_{37} = 0.033 \text{ SST} + 0.044$) is absolutely identical to the *E. huxleyi* equation of Prahl and Wakeham (1987) ($U^{K'}_{37} = 0.033 T + 0.043$) confirming its general applicability.

Cause for observed variability? Ecological, Genetic and Physiological Possibilities!



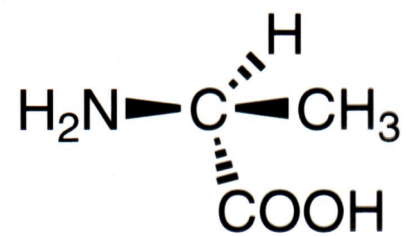
(Muller et al., 1998)

Indian Ocean Core (Bard et al., 1997)

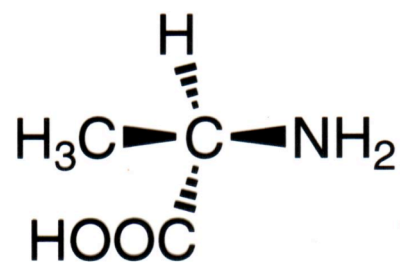


Aplicación 2. Racemización de amino ácidos

- Enantiómeros= estéreo isómeros en que la distribución espacial de sus átomos resulta en que una molécula es la imagen especular de la otra.
- Estéreo isómeros que no son imágenes especulares se llaman diasterómeros
- Amino ácidos son principalmente L(levorotatorios). Algunos son D(dextrorotatorios)



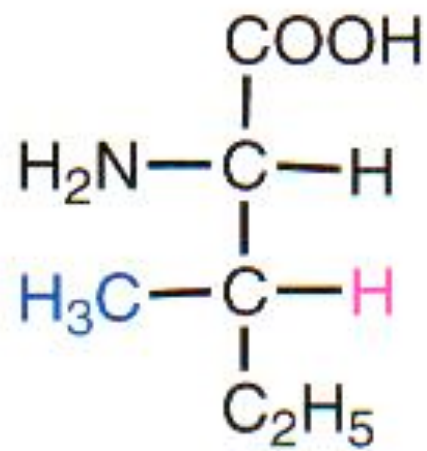
L-alanine



D-alanine

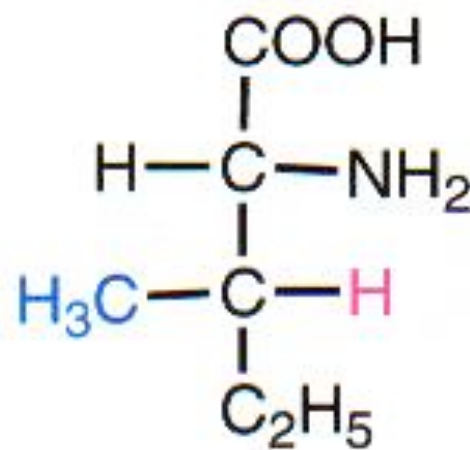
http://cwx.prenhall.com/petrucci/medialib/media_portfolio/text_images/083_Chirality.MOV

- Algunos amino ácidos como treonina e isoleucina contienen más de un carbono quiralico (4 átomos diferentes).
- Si ocurre inversión solo en el carbono alfa resulta en la formación de diasterómeros
- *Diasterómeros tienen propiedades químicas y físicas diferentes*

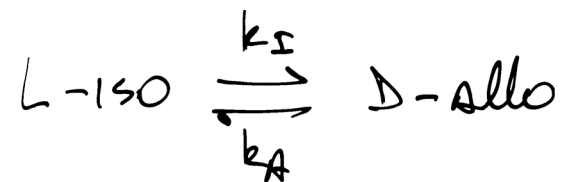


L-isoleucina

mirror



D-alloisoleucina



$$-\frac{dI}{dt} = k_I [I] - k_A [A]$$

$$\ln \left[\frac{1 + \left(\frac{A}{I} \right)}{1 - k^* \left(A/I \right)} \right]_t - \ln \left[\frac{1 + \left(\frac{A}{I} \right)}{1 - k^* \left(A/I \right)} \right]_{t=0} = (1 + k^*) \cdot k_I \cdot t$$

$$\frac{A}{I} = \text{ratio calcareous sediments} \quad k^* = \frac{1}{K_{eq}}$$

$$\left(\frac{A}{I} \right)_0 = \text{ratio recent sediment}$$

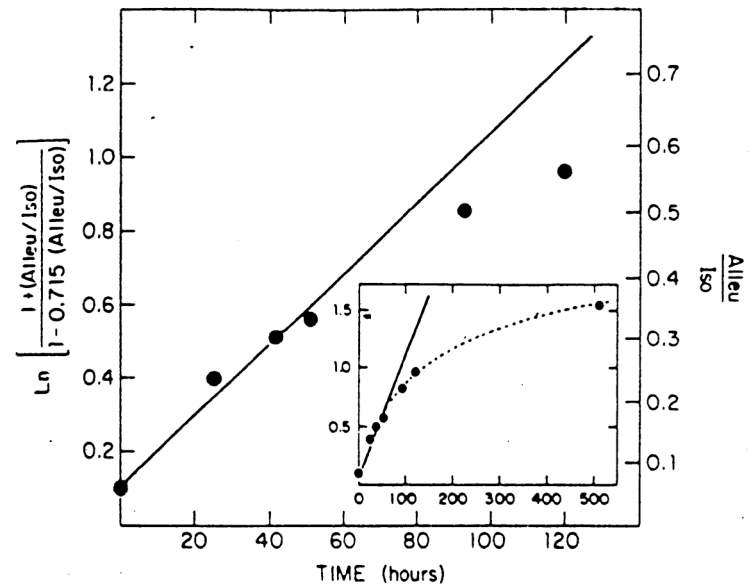


Fig. 1. Kinetics of conversion of isoleucine to alloisoleucine at 148.7°C in sediment from the 45–55 cm section of core CH96-G12. Reversible first-order kinetics are indicated by the solid line. This line was calculated using the average k_{iso} value obtained from the first three incubation periods. The value at $t = 0$ was determined by analysis of sediment from the 45–55 cm level that had not been heated, but which had been carried through the hydrolysis and desalting procedure. The insert shows a condensed version of the data included in order to show the value after 21 days (504 hr).

BADA & SCHROEDER (1972)
EARTH PLANET. SCI. LETT. 15, 1-11

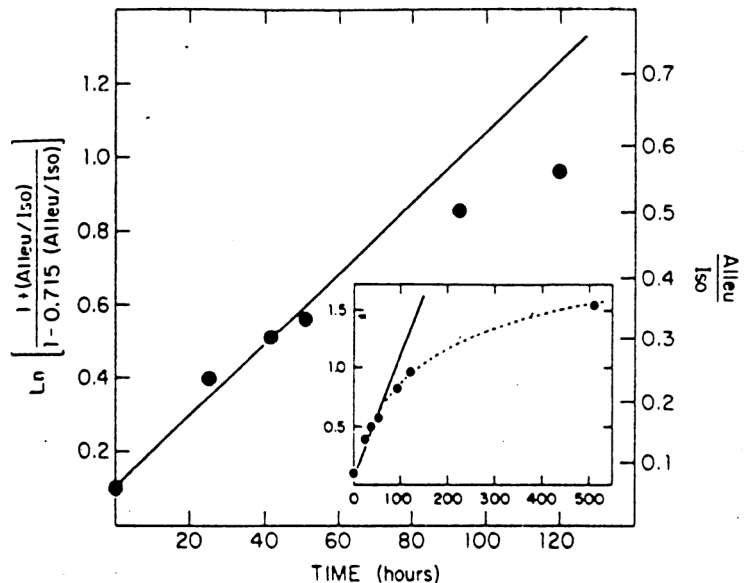


Fig. 1. Kinetics of conversion of isoleucine to alloisoleucine at 148.7°C in sediment from the 45–55 cm section of core CH96-G12. Reversible first-order kinetics are indicated by the solid line. This line was calculated using the average k_{iso} value obtained from the first three incubation periods. The value at $t = 0$ was determined by analysis of sediment from the 45–55 cm level that had not been heated, but which had been carried through the hydrolysis and desalting procedure. The insert shows a condensed version of the data included in order to show the value after 21 days (504 hr).

BADA & SCHROEDER (1972)
EARTH PLANET. SCI. LETT. 15, 1–11

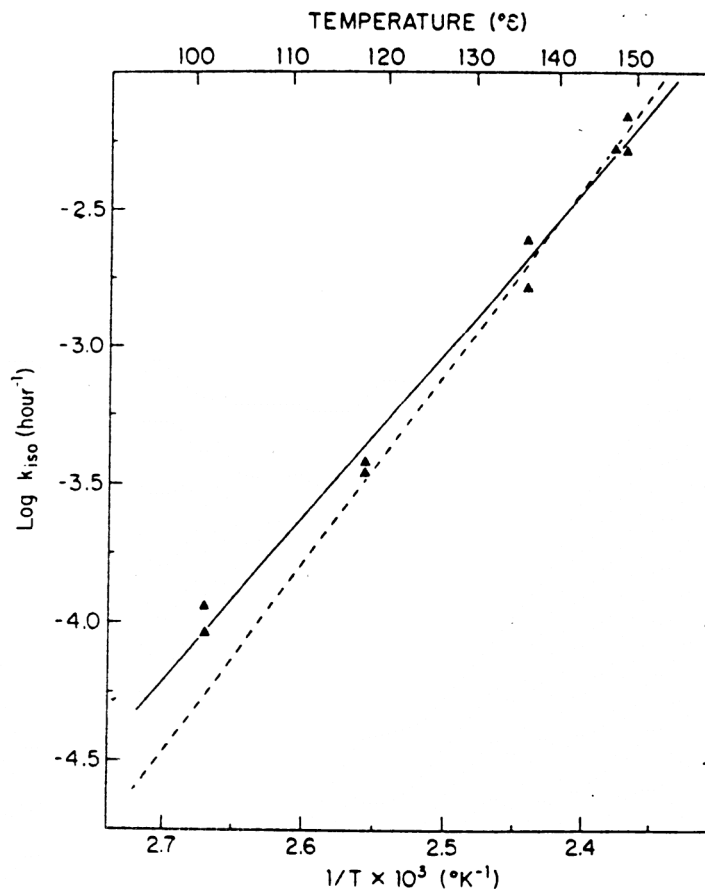


Fig. 2. $\log k_{\text{iso}}$ vs. $1/T$ ($^{\circ}\text{K}^{-1}$) for temperatures between 100° and 148°C ; ▲, values of $\log k_{\text{iso}}$ determined in the 25–35 and 45–55 cm levels of core CH96-G12. The solid line is a least squares fit of the CH96-G12 rate constants. The dashed line represents the rate constants for isoleucine buffered at pH 7.6 in aqueous solution (taken from ref. [5]).

$$k = Ae^{-E_a/RT}$$

Table 1
Amount of racemization of isoleucine in cores P6304-8 and P6304-9 and corresponding k_{iso} values.

Core and depth (cm) (foraminiferal fraction except as indicated)	Alleu/iso	$^{230}\text{Th}/^{231}\text{Pa}$ age (yr) ^b	$k_{iso} (\text{yr}^{-1})^c$	D/L AA
P6304-8, 320	0.222	91 000	2.2×10^{-6}	88,000
575-579 ^a	0.272	162 000	1.6×10^{-6}	152,000
P6304-9, 0	~0.02	-	-	
60	~0.07	19 000	$\sim 2.5 \times 10^{-6}$	18,000
190	0.154	56 000	2.3×10^{-6}	56,000
193-197 ^a	0.136	58 000	2.0×10^{-6}	55,000
330	0.220	95 000	2.2×10^{-6}	87,000
400	0.203	113 000	1.6×10^{-6}	110,000
540	0.278	150 000	1.7×10^{-6}	146,000
Ave $k_{iso} = 2.0 \times 10^{-6} \text{ yr}^{-1}$				

^a Total sediment hydrolysis.

^b Age estimated from least squares fit of data given in ref. [12].

^c Calculated from eq. (2). The value for $t = 0$ was estimated from the alleu/iso ratio of P6304-9, 0 cm. → 0.02